



Study on the Rheological Properties of Slate with Hard Structural Surface

Rui Wang, Mingli Zhu*

School of Energy Science and Engineering, Henan Polytechnic University, Henan, China

*Corresponding author: njzhu2004@163.com

ABSTRACT

It is of important significance for the stability of rock engineering to research the non-linear characteristic of rock creep under high stress. The shear creep behavior experimental of slate with hard structural plane were done by using CSS-283 two-way universal testing machine, to analysis on the variation law of creep parameters with stress and time, and obtained the nonsteady parameters creep equation. By the comparison with the theory calculated results of the stationary and non-stationary models and the test results, the non-stationary viscoelastic rheological model is the more exactly reflect the rock viscoelastic deforming performance than the stationary viscoelastic rheological models.

KEYWORDS

Non-Stationary Parameter; Shear Creep; Creep Model; Viscoelastic Deformation.

1. INTRODUCTION

In recent decades, with the rapid development of economic construction and the continuous expansion of construction scale, the development of underground space has been progressing deeper. Deeply buried rock masses exist within complex geological environments, characterized by unique structural features and high in situ stress. Therefore, studying the rheological characteristics of rock masses under high stress conditions is of significant importance.

Under high-stress conditions, the creep deformation of rock masses exhibits significant nonlinear characteristics. However, the elements used in traditional continuum theory are linear; thus, regardless of the number of elements or the complexity of their combinations, the resulting constitutive relations remain linear, which makes it impossible to study nonlinear rheology [1],[2]. Therefore, it is necessary to improve the existing framework to establish a nonlinear rheological model.

In recent years, many researchers have conducted studies on the rheological properties of geotechnical materials. Kang Hongpu et al. improved the basic mechanical elements based on experimental data and established a constitutive model suitable for the deformation and failure characteristics of surrounding rock in deep soft rock roadways[3]. Ji Dongliang et al. developed a creep damage model capable of describing the entire creep process of coal-rock, analyzing the effects of different disturbance energies on the creep failure of coal-rock[4]. Zhang Huifeng et al. studied the changes in rheological parameters of gangue backfill slurry with graded addition of gangue particles under Talbol continuous gradation, as well as the influencing factors[5]. Wang Xiaoyong et al. investigated the effects of fly ash content and slurry quality concentration on the rheological properties of gangue backfill slurry through rheological experiments[6]. Lü Aizhong et al. suggested

that the elastic modulus has an exponential function relationship with time and established a creep equation for a non-stationary viscoelastic model[7]. Xiong Shihu et al. proposed an unsteady viscoelastic-plastic rheological model that takes into account the effects of stress state[8]. Zhang Qiangyong et al. considered the creep damage degradation effect and viewed rheological parameters as non-stationary, suggesting that parameters gradually weaken over time, thereby establishing a variable-parameter creep damage constitutive model[9]. Xu Weiya et al. presented a Newtonian body with a nonlinear viscosity coefficient and established a viscoelastic-plastic creep model capable of simulating the three stages of nonlinear creep in rocks[10],[13]. Zhou Hongwei et al. developed a fractional-order three-element constitutive model for salt rock based on damage theory, utilizing classical three-element models and the theory of fractional calculus[14],[15]. Zhu Zhende et al. introduced the non-stationarity of creep parameters into the constitutive equations, establishing a non-stationary creep constitutive model based on fractional derivatives[16],[17]. Liu Jianfeng et al. improved and established a new fractional-order viscoelastic-plastic creep model[18]. Tang Hudan et al. studied the viscoelastic-plastic characteristics of marble under cyclic loading[19].

This paper is based on shear creep experiments of the rigid structural surfaces of slate, analyzing the variations in creep parameters with respect to stress and time. It introduces non-stationary parameters related to time and stress levels, proposing a non-stationary creep model.

2. EXPERIMENT

2.1. Sample Preparation

The rock samples containing rigid structural panels used in the experiment were prepared into three standard specimens measuring 150 mm × 150 mm × 150 mm, designated as S1, S2, and S3.

2.2. Experimental Equipment

The shear creep tests with graded loading on shale with rigid structural panels were conducted using CSS-283 two-way universal testing machine developed by the Changchun Testing Machine Research Institute (Fig. 1).

2.3. Experimental Method

Creep testing method using stepwise loading. The procedure is as follows:

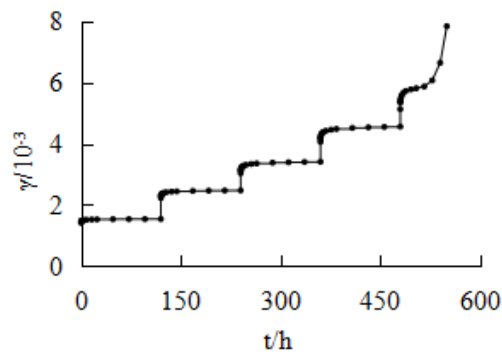
- (1) Apply axial stress, and once the displacement stabilizes, proceed with the application of shear stress. The axial stresses applied to slate specimens S1, S2, and S3 are 12 MPa, 18 MPa, and 24 MPa, respectively.
- (2) Apply shear stress and measure the shear displacement. Once the deformation stabilizes, apply the next level of shear stress, repeating the above steps until the slate specimen undergoes creep failure.



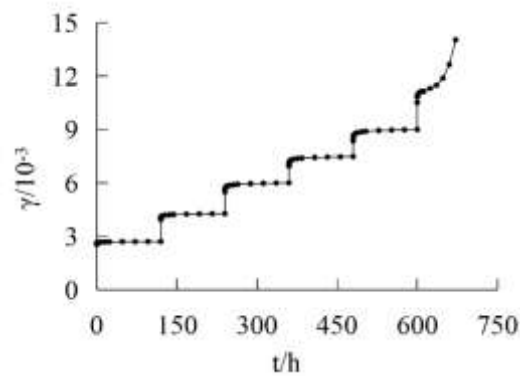
Fig. 1 CSS-283 two-way universal testing machine

3. ANALYSIS OF EXPERIMENTAL RESULTS

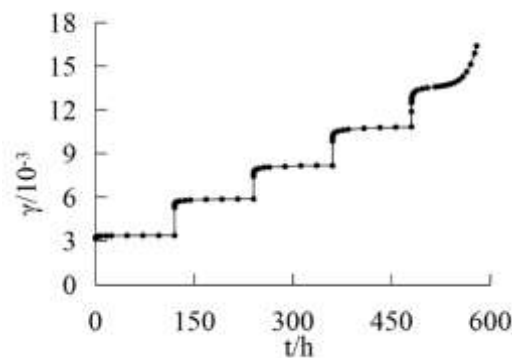
Through the stepwise loading creep tests on slate, the experimental curves for the three specimens are depicted as follows.



(a) $\sigma_n = 12 \text{ MPa}$ Slate S1



(b) $\sigma_n = 18 \text{ MPa}$ Slate S2



(c) $\sigma_n = 24 \text{ MPa}$ Slate S3

Fig. 2 Creep Curves of Shale Under Various Load Levels

From Fig. 2, Tangential strain (γ) and load application time (t) it can be observed that the shale specimens containing hard structural planes exhibit the following behaviors under constant normal stress:

(1) At the moment each level of shear stress is applied, the shale with hard structural planes experiences a certain amount of instantaneous shear displacement. As time progresses, the shear displacement gradually increases, demonstrating a significant time-dependent behavior;

- (2) When the shear stress reaches a critical value, there is a transition from the initial decaying shear creep phase to a stable shear creep phase;
- (3) The magnitude of instantaneous shear displacement in shale with hard structural planes is related to both the normal stress and the level of shear stress. Higher normal stress results in smaller instantaneous shear displacements under the same level of shear stress.

4. RHEOLOGICAL MODEL

Creep deformation of shale can be classified into instantaneous deformation, viscoelastic deformation, and viscoplastic deformation. From the structural perspective of creep deformation, a five-element Kelvin model can be employed (Fig. 3), with the creep equation represented by Equation 1. The simulation results and creep parameters are presented in Table 1.

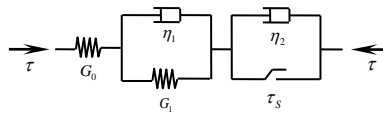


Fig. 3 Kelvin-Voigt Rheological Model

$$\begin{cases} \gamma = \frac{\tau}{G_0} + \frac{\tau}{G_1} \left(1 - e^{-\frac{G_1 t}{\eta_1}}\right) & \tau < \tau_s \\ \gamma = \frac{\tau}{G_0} + \frac{\tau}{G_1} \left(1 - e^{-\frac{G_1 t}{\eta_1}}\right) + \frac{\tau - \tau_s}{\eta_2} t & \tau > \tau_s \end{cases} \quad (1)$$

Table 1. Identification Results of Kelvin-Voigt Model Parameters for Shear Creep Tests on Shale

σ_n /MPa	τ /MPa	G_0 /GPa	G_1 /GPa	η_1 /GPa.h	η_2 /GPa.h/GPa.h	τ_s /MPa	Fitting error
12	1.7	1.182	20.01	47.02			0.0001
	3.4	1.513	17.48	45.83			0.0008
	5.1	1.709	13.87	40.87			0.0029
	6.8	1.761	11.17	34.77			0.0078
	7.8	13.07	1.771	0.001	17.25	7.2	0.0917
18	2.1	0.806	20.31	47.42			0.0002
	4.2	1.051	16.38	48.31			0.0017
	6.3	1.159	12.44	41.64			0.0064
	7.8	1.178	10.44	36.47			0.0134
	9.3	1.190	8.928	32.22			0.0248
	10.8	1.166	11.97	1.761	16.42	10.1	0.1005
24	3.15	0.977	21.98	43.50			0.0060
	6.30	1.178	12.86	34.12			0.0100
	8.67	1.214	9.329	30.14			0.0200
	11.03	1.213	7.247	25.91			0.0509
	13.40	1.112	12.30	3.551	73.03	12.5	0.1170

Based on Table 1, we can observe the following:

(1) At low stress levels, the steady-state viscoelastic model can adequately describe the creep behavior of slate, exhibiting a small fitting error. However, at high stress levels, the viscoelastic model fails to accurately capture the creep behavior of slate, resulting in a significant fitting error. This indicates that the steady-state parameters of the viscoelastic model are insufficient for accurately representing the creep characteristics of slate under high stress levels. Furthermore, the model does not accurately describe the creep failure process.

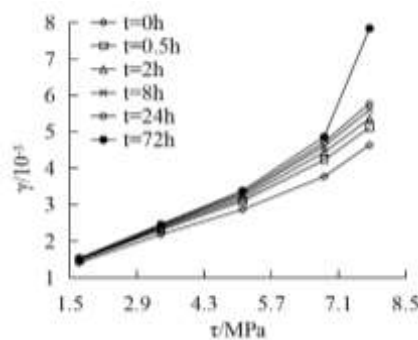
(2) The creep parameters (G_0), (G_1), and (η_1) of the viscoelastic model are all influenced by the magnitude of the load and time, exhibiting non-stationarity.

(3) The parameters of the viscoelastic model are constants that do not change with time or load. In practice, to achieve a better fitting result, different parameter values are often employed at varying shear stress levels. Consequently, the number of parameters tends to increase significantly with the escalation of load levels, and the parameters for each group can differ substantially, presenting challenges in parameter selection for engineering applications.

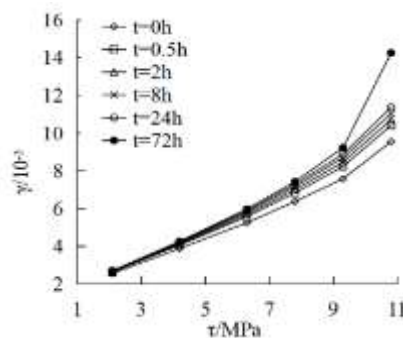
5. RESEARCH ON THE NONLINEAR VISCOELASTIC MODEL OF SLATE

5.1. Nonlinear Shear Viscoelastic Characteristics of Slate

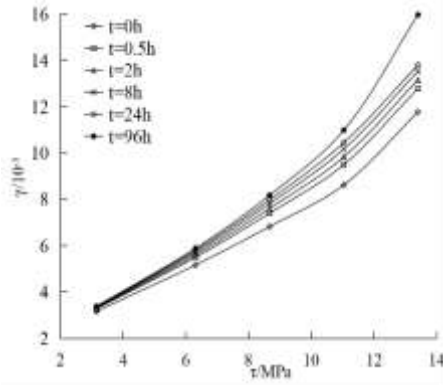
Fig. 4 illustrates the stress-strain isochrones of shear creep for the hard structural surfaces of slate. It is evident that the isochrones at different times are not straight lines, indicating that creep behavior is nonlinear. Furthermore, as time progresses and the stress level increases, the deviation of the isochrones from linearity also becomes more pronounced. This suggests that the degree of nonlinearity in creep behavior intensifies with increasing stress levels and over time. If linear viscoelastic theory is employed to study the creep behavior of rocks, it will ultimately reflect only linear viscoelastic-plastic properties, failing to capture the inherent nonlinear characteristics of the rock. Therefore, treating the creep parameters as non-stationary, determined through creep tests, and subsequently conducting nonlinear analytical calculations is considered an ideal approach, adhering to rigorous academic standards[2].



(a) $\sigma_n=12\text{MPa}$ Slate S1



(b) $\sigma_n=18\text{MPa}$ Slate S2



(c) $\sigma_n=24\text{MPa}$ Slate S3

Fig. 4 The isochronous stress-strain curves of slate under various loading levels.

5.2. Research on the Non-Stationary Characteristics of Viscoelastic Parameters

The instantaneous elastic shear modulus (G_0) represents the magnitude of instantaneous elastic deformation, while the viscoelastic shear modulus (G_1) represents the magnitude of viscoelastic deformation, both of which are time-independent. The viscosity coefficient (η_1) is considered a non-steady variable ($\eta_1(t)$), which changes over time. The viscoelastic deformation can be expressed as:

$$G_1\gamma + \eta_1(t)\dot{\gamma} = \tau \quad (2)$$

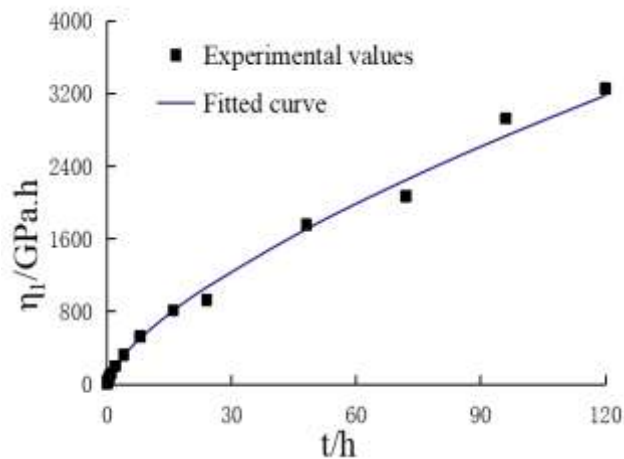
Solving the equation yields:

$$\gamma = e^{-\int \frac{G_1}{\eta_1(t)} dt} \cdot \left(\int \frac{\tau}{\eta_1(t)} e^{\int \frac{G_1}{\eta_1(t)} dt} dt + c \right) \quad (3)$$

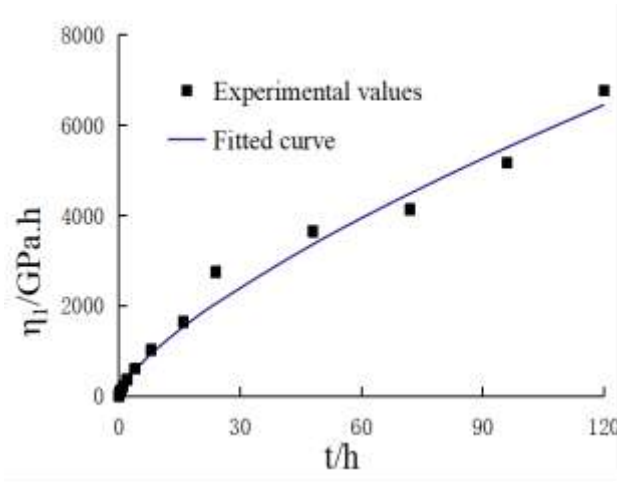
The relationship between the viscosity coefficient and time (as shown in Fig. 5) can be represented by a power function as follows:

$$\eta_1(t) = At^B \quad (4)$$

In the equation, (A) and (B) are the material parameters of the rigid structural surface of the slate, with the fitting results illustrated in Fig 5.



(a) $\tau = 6.30\text{MPa}$ ($\sigma_n=18\text{MPa}$)



(b) $\tau = 8.67\text{MPa}$ ($\sigma_n=24\text{MPa}$)

Fig. 5 The relationship between the viscoelastic coefficient and time.

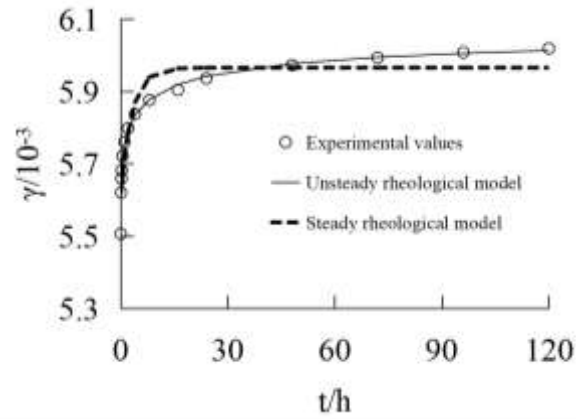
Therefore, the total elastic deformation can be expressed as:

$$\gamma_e = \frac{\tau}{G_0} + \frac{\tau}{G_1} \left(1 - e^{\frac{-G_1 t^{1-B}}{A(1-B)}} \right) \quad (5)$$

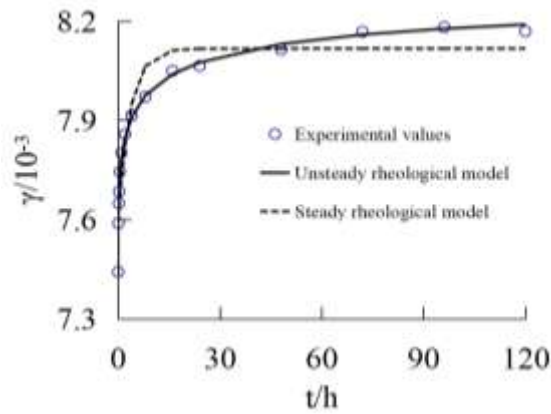
Based on Equation (5), the elastic rheological parameters of the slate were inverted from the results of indoor shear creep tests on slates containing structural planes, yielding the creep parameters presented in Table 2.

Table 2. Identification results of the viscoelastic parameters for the non-steady state rheological model.

σ_n/MPa	τ/MPa	G_0/GPa	G_1/GPa	$A/\text{GPa.h}$	B	Fitting error
12	1.7	1.409	19.74	73.66	0.626	0.00008
	3.4	1.934	27.24	101.6	0.635	0.00011
	5.1	2.241	31.78	118.6	0.640	0.00015
	6.8	2.420	34.54	128.9	0.645	0.00021
18	2.1	0.922	21.00	80.51	0.663	0.00007
	4.2	1.266	28.83	110.5	0.672	0.00009
	6.3	1.437	32.28	123.7	0.681	0.00013
	7.8	1.470	33.48	128.3	0.684	0.00017
	9.3	1.499	34.16	130.9	0.689	0.00021
24	3.15	1.141	41.21	162.9	0.702	0.00010
	6.30	1.442	52.09	205.7	0.705	0.00014
	8.67	1.515	54.25	214.6	0.714	0.00019
	11.03	1.532	55.31	218.8	0.721	0.00023



(a) $\tau = 6.30\text{MPa}$ ($\sigma_n=18\text{MPa}$)



(b) $\tau = 8.67\text{MPa}$ ($\sigma_n=24\text{MPa}$)

Fig. 6 Comparison of the fitting curves of the steady-state and non-steady-state rheological models with the experimental curves.

Fig. 6 presents a comparison between the fitting curves of the steady-state and non-steady-state rheological models and the experimental curves. It is evident that the fitting curve of the steady-state rheological model shows a poor agreement with the experimental curve, particularly during the stable stage of creep, where the shear displacement creep rate of the fitting curve becomes zero, resulting in a horizontal line on the graph, which does not match the experimental results. In contrast, the non-steady-state rheological model, which takes into account the time-dependent characteristics of the viscosity coefficient, provides a better fit to the experimental curve.

5.3. Variation of instantaneous elasticity and viscoelastic parameters with stress levels.

From Table 2, it can be observed that the instantaneous shear modulus (G_0), the viscoelastic shear modulus (G_1), and the coefficient A all increase with an increase in shear stress, exhibiting similar trends. Therefore, it is assumed that the variation of the instantaneous shear modulus (G_0), the viscoelastic shear modulus (G_1), and the coefficient A with stress levels follows the same pattern, and can be uniformly represented as $(D(\tau))$. (D_0) represents the initial value of the parameter. The variation of $(D(\tau))$ with shear stress can be expressed as:

$$D(\tau) = D^0(1 - P_1 \exp(P_2 \tau)) \quad (6)$$

The total elastic deformation can be expressed as:

$$\gamma_e = \frac{\tau}{G_0^0(1 - P_1 \exp(P_2 \tau))} + \frac{\tau}{G_1^0(1 - P_1 \exp(P_2 \tau))} \left(1 - e^{\frac{-G_1^0 t^{1-B}}{A(1-B)}} \right) \quad (7)$$

Based on the derived Equation (7), the results from the indoor shear creep tests on structurally intact slate panels were utilized to perform an inversion analysis of the rheological elastic parameters of the slate. The goodness of fit of the regression was assessed using correlation coefficients. The inverted rheological parameters and their corresponding correlation coefficients are presented in Table 3.

Table 3. Identification results of deformation parameters from shear creep tests on slate

σ_n /MPa	G_0^0 /GPa	G_1^0 /GPa	A/GPa.h	B	P1	P2	Correlation index
12	2.67	38.8	145	0.637	0.813	-0.317	0.93
18	1.61	39.1	134	0.678	0.907	-0.389	0.96
24	1.54	55.6	220	0.711	1.067	-0.446	0.95

5.4. Unsteady viscosity coefficient of the third stage creep

Numerous creep tests have confirmed that when the applied stress exceeds the long-term strength of the rock, the creep process will enter the third stage of creep (accelerated creep) as long as the duration is sufficiently long. During this stage, the viscosity coefficient decreases over time. Furthermore, the reduction in the viscosity coefficient is related to the magnitude of the applied stress; specifically, the greater the applied stress, the smaller the viscosity coefficient. Sun Jun et al. proposed a relationship for the time-dependent viscosity coefficient [2]:

$$\eta_2(\tau, t) = \frac{\eta_2^0 e^{-(\tau - \tau_\infty)kt}}{1 + (\tau - \tau_\infty)kt} \quad (8)$$

The relationship for the time-dependent viscoplastic deformation:

$$\gamma_{vp}(\tau, t) = \frac{(\tau - \tau_\infty)}{\eta_2^0} t e^{(\tau - \tau_\infty)kt} \quad (9)$$

(k) is a constant determined from creep tests; (η_2^0) is the initial viscosity coefficient; and (τ_∞) is the long-term strength of the rock.

The accelerated creep data for slate were simulated, and the simulation results along with the creep parameters are presented in Table 4.

Table 4. Results of parameter identification for the third stage of creep deformation in slate.

σ_n /MPa	η_2 /GPa	τ /GPa	k	Correlation index
12	3.75	7.21	0.131	0.92
18	2.93	10.08	0.051	0.90
24	2.09	12.53	0.065	0.89

5.5. Nonsteady state shear rheological model for slate.

The nonsteady-state creep equation can be expressed as:

$$\begin{cases} \gamma = \frac{\tau}{G_0^0 d(\tau)} + \frac{\tau}{G_1^0 d(\tau)} \left(1 - e^{-\frac{G_1^0 t^{1-B}}{\eta_1}}\right) & \tau \leq \tau_\infty \\ \gamma = \frac{\tau}{G_0^0 d(\tau)} + \frac{\tau}{G_1^0 d(\tau)} \left(1 - e^{-\frac{G_1^0 t^{1-B}}{\eta_1}}\right) + \frac{\tau - \tau_\infty}{\eta_2^0} t e^{(\tau - \tau_\infty)kt} & \tau > \tau_\infty \end{cases} \quad (10)$$

Fig. 7 illustrates the comparison of shear creep test data for slate at a normal stress of $\sigma_n = 12$ MPa, along with the nonsteady-state rheological model and the steady-state model. From the figure, it can be concluded that: (1) the nonsteady-state parameter rheological model provides a good fit at both low and high stress levels; (2) the nonsteady-state parameter steady-state model effectively describes the creep process during the third stage of loading, exhibiting not only a small error in creep deformation but also a trend that is largely consistent with the experimental curve.

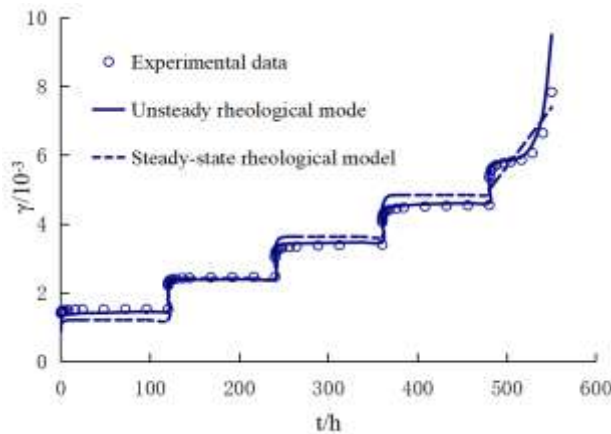


Fig. 7 Comparison of Slate Creep Test Data, Nonsteady-State Rheological Model and Steady-State Model ($\sigma_n = 12$ MPa)

6. SUMMARY

Through shear creep tests on slate containing hard structural surfaces using the CSS-283 biaxial creep testing machine, along with an analysis of the preliminary inversion results of the steady-state

viscoelastic model, this study investigates the non-stationary characteristics of the rheological parameters and proposes a shear creep model incorporating non-stationary parameters. The main conclusions of this paper are as follows:

- (1) The steady-state viscoelastic model cannot capture the nonlinear characteristics of rheological deformation. The nonlinear characteristics of rheology inevitably lead to non-stationary properties of the rheological parameters.
- (2) During the shear creep process of slate, the instantaneous shear modulus (G_0), the viscoelastic shear modulus (G_1), and the viscosity coefficient (η_1) are all dependent on the magnitude of the shear stress, while the viscosity coefficient (η_1) is also related to the creep duration. As the shear stress increases, the instantaneous shear modulus (G_0), the viscoelastic shear modulus (G_1), and the viscosity coefficient (η_1) all increase. The viscosity coefficient (η_1) tends to increase with time.
- (3) The non-stationary rheological model, which takes into account the non-stationary characteristics of the parameters, more accurately reflects the rheological deformation characteristics of rock masses compared to the steady-state rheological model.

REFERENCES

- [1] SUN Jun. Rheology of geotechnical materials and its engineering application[M]. Beijing: China Architecture & Building Press, 1999.
- [2] SUN Jun. Some advances in the study of rock rheological mechanics and its engineering applications[J]. Chinese Journal of Rock Mechanics and Engineering, 2007(6): 1081–1106.
- [3] KANG Hongpu, YI Kang. Simulation study on dilatant and rheologic properties of soft rocks surrounding deep roadway and its application[J]. Journal of China Coal Society, 2023, 48(1): 15-33.
- [4] JI Dongliang, CHENG Hui, ZHAO Hongbao, et al. Creep damage evolution and instability induction mechanism of rock under impact disturbance[J]. Journal of China Coal Society, 2024, 49(S1): 197–207
- [5] ZHANG Huifeng, LU Cheng, ZHANG Side, et al. Study on the Rheological Characteristics of Backfill Slurry with Grade Addition of Gangue Particles[J]. Nonferrous Metals Engineering, 2024, 14(10): 116-123.
- [6] WANG Xiaoyong, WANG Zhaoming, XU Hailong, et al. Rheological Properties and Consolidation Mechanism of Cement-Fly Ash Cemented Gangue Backfill Material[J]. Nonferrous Metals Engineering, 2024, 14(6): 134-143.
- [7] LÜ Aizhong, DING Zhikun, JIAO Chunmao, et al. Identification of non-stationary creep constitutive models of rock[J]. Chinese Journal of Rock Mechanics and Engineering, 2008, 27(1): 16-21.
- [8] XIONG Shihu, ZHOU Huoming, HUANG Shuling, et al. Rheological model of soft rock in Goupitan by in-situ plate-loading creep tests[J]. Chinese Journal of Geotechnical Engineering, 2016, 38(1): 53–57.
- [9] ZHANG Qiang-yong, YANG Wen-dong, ZHANG Jian-guo, et al. Variable parameters-based creep damage constitutive model and its engineering application[J]. Chinese Journal of Rock Mechanics and Engineering, 2009, 28(4): 732-739.
- [10] ZHANG Yu, JIN Peijie, XU Weiya, et al. Experimental study of triaxial creep behavior and long-term strength of clastic rock in dam foundation[J]. Rock and Soil Mechanics, 2016, 37(5): 1291-1300.
- [11] ZHANG Yu, XU Weiya, WANG Wei, et al. Study of rheological tests and its parameters identification of soft rock in fractured belt[J]. Chinese Journal of Rock Mechanics and Engineering, 2014, 33(Supp.2): 3412-3420.
- [12] XU Weiya, HUANG Wei, ZHANG Tao, et al. Experimental study on rheological properties of layered rock mass with soft interlayers[J]. Journal of Hohai University(Natural Sciences), 2020, 48(4): 327-333.
- [13] XU Weiya, NIE Weiping, ZHOU Xianqi, SHI Chong, WANG Wei, FENG Shurong. Long-term stability analysis of large-scale underground plant of Xiangjiaba hydro-power station[J]. Journal of Central South University of Technology, 2011(18): 511-520.
- [14] DING Jingyang, ZHOU Hongwei, LIU Di, et al. Research on fractional derivative three elements model of salt rock[J]. Chinese Journal of Rock Mechanics and Engineering, 2014, 33(4): 672–678.
- [15] ZHOU H W, WANG C P, HAN B B et al. A creep constitutive model for salt rock based on fractional derivatives[J]. International Journal of Rock Mechanics and Mining Sciences, 11, (1): 6-21.
- [16] HE Zhilei, U Zhende, ZHU Mingli, et al. An unsteady creep constitutive model based on fractional order derivatives[J]. Rock and Soil Mechanics, 2016, 37(3): 737–744, 775.

- [17] Zhu Zhende, Zhu Mingli, Ruan Huaining, et al. Nonlinear creep model of surrounding rock of long, large and deep tunnel[J]. *Rock and Soil Mechanics*, 2011, 32(Z2): 27-35, 69.
- [18] WU Fei, XIE Heping, LIU Jianfeng, et al. Experimental study of fractional viscoelastic-plastic creep model[J]. *Chinese Journal of Rock Mechanics and Engineering*, 2014, 33(5): 964–970.
- [19] Hu-dan Tang, Ming-li Zhu, Zhen-hua Li. Microstructure size and packing of fracture surface on the nonlinear breakage mechanical response of different marbles under cyclic loading[J]. *Engineering Geology*, 2024, 337(107572)